ACS OMEGA

Open Access

http://pubs.acs.org/journal/acsodf

Article

Thermodynamic Insights into Variation in Thermomechanical and Physical Properties of Isotactic Polypropylene: Effect of Shear and Cooling Rates

Ahmad S. Jawed, Mohd Nasir Khan, Naseem A. Khan,* Mohammed A. Hakeem, and Parvez Khan*

Cite This: *ACS Omega* 2023, 8, 36775−36788

Read Online

ACCESS | Metrics & More | Article Recommendations

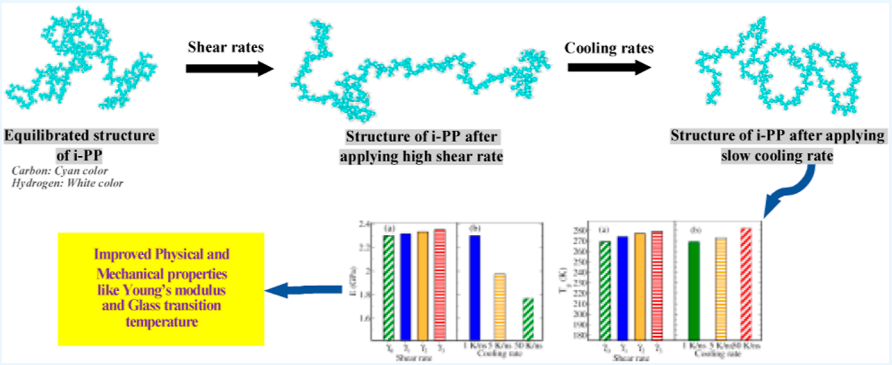

ABSTRACT: In order to elucidate the effect of shear and cooling process on structural, thermomechanical, and physical properties of polymer melt, excess entropy, a thermodynamic quantity is calculated from radial distribution function generated from equilibrated parts of the molecular simulation trajectories. The structural properties are calculated, which includes the density of polypropylene melt, end to end distance, radius of gyration of the polypropylene polymer chain, and monomer−monomer radial distribution function. Non-equilibrium molecular dynamics simulation was employed to investigate the role of the applied shear rate on the properties of polypropylene. Furthermore, a range of cooling rates were employed to cool the melt. Thermomechanical properties, such as Young's modulus, and physical properties, such as glass transition temperature, were determined for different cases. Results showed that slow cooling and high shear substantially improved the Young's modulus and glass transition temperature of the i-PP. Furthermore, a two-body contribution to the excess entropy was used to elucidate the structure−property relationships in the polymer melt as well as the glassy state and the dependence of shear and cooling rate on these properties. We have used the Rosenfeld excess entropy−viscosity relationship to calculate the viscous behavior of the polymer under a steady shear condition.

1. INTRODUCTION

Today, it is well-accepted that the complex flow behavior of polymeric liquids emerges from the large range of time and length scales that describe the morphology of these systems.[1] Also, to achieve the target for technological or industrial requirements in polymer engineering, it is largely depends on the manipulation of mechanical and thermal properties of the polymer.[2] Therefore, predicting the behavior of polymeric systems to an applied shear rate requires a fundamental understanding of the mechanism that occur across various time scales.[3,4] Focusing, in particular, the rate of cooling and the applied shear rate are the two main factors that influence the industrial process of producing the polymer end-products. This explains why many experimental studies have been conducted in the past to examine the effect of the above-mentioned factor (shear rate and cooling rate) on various morphological properties of the polymers.

Isotactic polypropylene (i-PP), a thermoplastic semicrystalline polymer with high consumption due to its well-balanced physical and mechanical properties and outstanding processing efficiency at a low cost, has been the most inventive and fastest growing polymer. Semi-crystalline characteristic and tunable properties of i-PP make it suitable for automobile, packaging, consumer goods, fibers, and medical industries.[5,6] The alpha (α) form of i-PP is often exposed to shear flow and cooling process during processing that accelerates the morphological changes in the polymer structure that leads to the improve-

Received: May 15, 2023
Accepted: August 24, 2023
Published: October 2, 2023

ment in the properties of the end-product,[7] and this became the motivation behind choosing the α form of i-PP in the current simulation study.

For instance, in injection molding, high shear rate and rapid cooling near the mold wall combine to produce highly oriented layers close to the surface. The temperature affects the rate of morphological changes during the production process of polymer with the fastest rate occurring in the temperature range between the glass transition temperature (T_g) and melting temperature (T_m).[8,9] Scientists and researchers have become increasingly interested in studying the morphology of polymers during the past few years, and sufficient work is still being put into this field of study.[10,11] Many researchers have examined the mechanical characteristics of i-PP using experimental techniques such as wide-angle X-ray scattering, electron microscopy etc.,[12] and concluded that the crystal phase, its molecular weight, and the spherulite size are the important factors to decide the mechanical properties of semi-crystalline polymers. Guan et al. has studied the structural, thermodynamic, and kinetic behavior of various chain lengths of polypropylene during the heating and cooling process. The results showed that the remarkable stability of amorphous PP1000−PP3000 is due to low molecular mobility and large entropy.[13]

Effective transition from design to production of engineering materials, such as polymers, is typically a time-consuming and costly process that necessitates an iterative search for a specific microstructure to meet targeted properties while balancing various constraints such as material availability, manufacturability, and production cost. The significance of computers in materials design has grown significantly in recent decades owing mostly to the rapid expansion of computing power and more precise and efficient computational algorithms. Nowadays, computing methodologies are routinely utilized to develop knowledge and anticipate diverse material properties. The bottom-up approach of large-scale phenomena in polymers needs effective simulation techniques, for instance, molecular dynamics (MD) simulations. Such simulations will not only help us understand structure−property relationships but also allow us to pick and optimize fundamental components to improve their attributes and maximize their performance. Furthermore, analyzing the mobility of individual molecules as well as their individual atomic segments under flow is necessary to comprehend the physical processes that take place on various time scales. Without a doubt, MD simulations serve a critical role in aiding the understanding of atomic-level experimental data. However, it is important to keep in mind that, in comparison to the number of degrees of freedom inside molecular systems of interest, experimental data are typically relatively restricted.[14] Molecular simulations using non-equilibrium MD (NEMD) offers a practical alternative to experiment by allowing important calculations of morphological and configurational features of the molecular system.[15] Additionally, these computational investigations offer meaningful interpretations and explanations of microscopic and macroscopic features of materials that have been experimentally observed. With more computational power, MD simulations can, therefore, aid in the design and development of new materials. The below paragraphs discuss how different researchers have investigated the properties of polypropylene by looking at its density, radius of gyration, self-diffusivity, glass transition temperature, and Young's modulus.

Determination of the dynamical property (e.g., self-diffusion coefficient) of polymer using molecular simulation techniques has been used in recent times. The simulation study of polypropylene melt using Monte Carlo simulation (M_w = 9900 g/mol) by Ernst[16] reveals that the relative magnitude of the rate of diffusion follows the amount of molecular weights which indicates that the molecular weight effect dominates the stereochemical effect in the simulation. Logotheti et al. has developed an atomistic model to find out the properties of isotactic PP melts using MD simulation in the isothermal−isobaric (NPT) ensemble and calculates the structural, dynamical, volumetric, and conformational properties of i-PP having a degree of polymerization 76 (molecular mass: 3208 $\frac{g}{mol}$). Dynamic behavior was investigated by systematically mapping the atomistic MD trajectories onto the Rouse model. The normal-mode analysis confirmed that the Rouse model accurately describes long length scale chain dynamics, and the value of self-diffusion coefficient were also calculated from the mean square displacement (MSD) of the chain centers of mass in the long-time.[17]

In the past decade, some molecular simulation studies have been conducted to understand the mechanical behavior of i-PP. For example, Qian and Ludovice[18] calculated the density and Young modulus of i-PP under various operating circumstances using the constant stress MD approach. However, this strategy was hampered by the inherently small-time scale. Furthermore, Boland et al.,[19] studied polypropylene's morphological and dynamical properties. In another work, Kitamura et al.,[20] examined the elasticity of polypropylene under various temperatures and strain rates. In addition, they suggested the Mises and Tresca criterion to calculate the yield stress in the uniaxial and biaxial stress states. In a recent study, Kim et al.,[21] used experiment and molecular simulation to study the impact of initial crystallinity and operating temperature on the mechanical characteristics of the i-PP polymer. Simulation models were built by using a combination of crystalline and amorphous layers to adjust the degree of crystallinity. According to their findings, as temperature increased, the elastic modulus of the i-PP models decreased, whereas the yield strength and Young's modulus enhanced as crystal concentration increased.

Glass transition temperature (T_g), the most significant single descriptor of semicrystalline polymers, is another crucial polymer physical characteristic. The type of usage for a polymer is determined by the value of this parameter. It is anticipated that the selection and design of novel materials would greatly benefit from the ability to precisely estimate values of T_g from the chemical structure of the polymer through simulations. Han et al.[22] were the first who used molecular simulation approach to calculate the T_g of several amorphous and semi crystalline polymers using $v-T$ curves obtained from MD simulation data. Subsequently, Yu et al., investigated the role of chain flexibility and side groups on glass transition of polymers using all atom simulation.[23] They concluded that key roles are played in the glass transition process by energy elements like torsion energy and nonbonded energy. Furthermore, Yang and co-workers[24] investigated the various glass transition properties of atactic polypropylene bulk and freestanding thin films. Glass transition temperature was reported to be 364 K, which is significantly higher than the value reported in experimental studies.

https://doi.org/10.1021/acsomega.3c03378
ACS Omega 2023, 8, 36775−36788

However, the above studies predicted a considerably higher value of T_g. This was probably due to the very fast cooling rates employed in MD simulations compared to experiments. Further experimental studies revealed that very fast cooling rates significantly increased the apparent T_g value.[25,26] Han et al.[22] concluded that the T_g values calculated in simulation using the $v-T$ graph would still be relatively high in comparison to normal experiments even if MD simulations accurately depict the equilibrium melt and the start of vitrification at this time scale.[22] Therefore, the well-known Williams−Landel−Ferry (WLF) equation was recommended in some research to shift T_g to experimental cooling rates in order to account for the fast cooling observed in the MD simulations. In a recent MD study of starch, the T_g obtained from simulation was scaled using this equation to the T_g determined at an experimental cooling rate.[27]

Due to the difficulties in directly calculating the transport properties of soft matter systems, alternative techniques for their estimation have developed. One approach is to establish relationships between transport properties and thermodynamic parameters.[28] Rosenfeld worked in this direction and derived the relationship between reduced viscosity and excess entropy which depends on the argument that shows a macroscopic description of the soft matter systems like polymers.[29,30] Voyiatzis et al. investigated whether the transport properties of a real polymer scale with its excess entropy. In their simulation study, four unentangled polyethylene systems (no chains equals 25, 50, 100, and 150) over wide temperature ranges were considered and they look at the scaling of global transport properties like viscosity and diffusion coefficients, as well as segmental ones like bond and torsional relaxation times. They have concluded that the Rosenfeld relationship is a much better approach for polymer chains in melt state (Rouse regime).[31,32] Rondina et al. further investigated the link between the acceleration of dynamics caused by coarse-graining and the corresponding changes in excess entropy across different coarse-grained resolutions. Their findings for bead-spring models of polymer at various resolutions showed that the impact of coarse-graining in chain dynamics can be connected with the change in excess entropy for unentangled polymer melts, not just fluids of small molecules or hard sphere models, as previously discussed.[33]

By manipulating certain parameters like glass transition temperature (T_g) and Young's modulus, we can improve the end use as T_g and Young's modulus of i-PP can be tuned by cooling/annealing and shear flow rates. For example, in an experimental study, Koscher and Fulchiron, showed that Young's modulus of i-PP can be improved by increasing the shear rate.[34] Moreover, Kalay and Bevis demonstrated an increase in Young's modulus from 2079 to 2600 MPa for moldings generated via shear-controlled orientation injection molding process.[35] Generally, shear flow can cause several unique phenomena in polymeric or macromolecular liquids, such as phase transitions, strain hardening, replication, crystallization, and melting point increases.[36] Despite major breakthroughs in experimental technique development over the years, an explanation of these phenomena in terms of the microscopic processes following flow applications remains elusive. NEMD simulations offer a viable path in this direction since they allow one to track dynamics over a range of time scales (from times corresponding to the motion of individual monomers to times corresponding to the dynamics of entire chains). As a result, it is not surprising that much effort has been expended in recent decades to develop rigorous NEMD algorithms guided by non-equilibrium statistical mechanics principles, appropriate boundary conditions for systems subjected to elongation, and shear consistent with those encountered in real experiments.[37] We note that many investigations have been done on simple model polymers like polyethylene, leaving many other polymers (e.g., polypropylene and polystyrene) with more complex chemical structures relatively unexplored. Therefore, MD simulation techniques are employed in this work to study the effect of different shear and cooling rates on the microscopic behavior of the α form of i-PP as only few studies have been conducted in the past.

The crystallization process in i-PP is generally known to be sluggish, and most of the time polymer remains in semi crystalline morphology even under processing conditions. Generally, polymers do not crystallize easily upon cooling to the solid state as this requires substantial long-range ordering of the highly coiled and entangled chains present in the liquid state. Essential conditions for the onset of crystallization are the presence of high-density active nuclei or the availability of a crystal structure at the substrate surface. In this study, we are not considering any presence of active nuclei. Therefore, for the sake of simplicity here, we are considering only the ordered structure formation during the shear and cooling process. However, it is quite possible that the crystal content in the system will enhance. As observed in experiments, processing conditions substantially alter the structural, mechanical, and physical properties of the polymer. Here, we anticipated a local ordering of the polymer under processing conditions that leads to changes in the properties of the polymer. To control the qualities of products, it is crucial to understand this local ordering or rearrangement of the polymer chains. This is a very practical aspect of this work. In this work, one of the aims is to examine how the structural, mechanical, and physical characteristics of polymers vary when shear and cooling is applied. Furthermore, we investigated the thermodynamic changes behind these variations that can be helpful in understanding the process much better.

In this study, we employed a thermodynamic approach, wherein we utilize the two-body contribution to the excess entropy to elucidate the influence of shear flow and cooling rates on structural, thermomechanical, and physical properties of i-PP. It is widely accepted that shear flow and cooling rates have a significant impact on physical properties of polymer. To understand this, we performed NEMD simulation to incorporate the shear flow. Particularly, three distinct shear rates were used, which is followed by quick, medium, and slow melt cooling. The density, radius of gyration, and end-to-end distance were calculated at three different shear rates and cooling rates, which accounts for the structural property of i-PP. Moreover, to comment on the structural properties of i-PP melts, the monomer−monomer radial distribution function (RDF) $g(r)$, which is informative about intermolecular correlations and bulk packing, was calculated around the center carbon attached to the functional group. To look into the dynamics of i-PP, the self-diffusion coefficient is calculated at 450 K from the MSD curve. Thermal properties such as a glass transition are important in selecting materials for end-use applications. The transition from glassy (amorphous) solid to rubbery (viscous liquid) occurs at T_g, which is affected by a variety of factors such as structural changes in molecules due to shear flow and cooling rate which is studied in this research

https://doi.org/10.1021/acsomega.3c03378
ACS Omega 2023, 8, 36775−36788

work. Furthermore, Young's modulus (E_i) for the frozen structures of i-PP was determined from a series of deformation simulations in which strain was applied by stepwise uniaxial extension or compression. In addition, Rosenfeld excess entropy−viscosity relationship is utilized to investigate the viscous behavior of polymer melt under a steady shear condition.

2. METHODS

2.1. Model Systems and Initial Preparation. The aim of this work is to understand the thermodynamics of variation in thermomechanical and physical properties of polymer under processing conditions using MD as well as NEMD simulations. We use i-PP polymer (molar weight of 4200 g/mol) chains having 100 repeating units $\{CH_2CH(CH_3)\}$. To enable sampling of equilibrium trajectories in an acceptable amount of simulation time, the molecular weight of i-PP was chosen to be just below the entanglement length. The methods to prepare the initial structures of i-PP have been described in our previous work.[38] All MD simulations were performed using the GROMACS-2020.4 MD simulator.[39,40] For all-atomistic simulations, we have used CHARMM36 FF.[41,42] Initially, a single i-PP chain was equilibrated in the vacuum. Furthermore, PACKMOL software was used to pack 40 polymer chains in a box. For all simulations, a time step of 2 fs was used and a threshold of 1.2 nm was used for VdW interaction with a force-shift of 1.0 nm, while PME $\left(\text{accuracy}10^{-2}\ \frac{\text{kcal}}{\text{mol}}\right)$ was used for long-range Columbic interactions. Then, the i-PP melt which consists of 40 chains of polymer was equilibrated at 450 K. Most populated equilibrated structures of i-PP were used to prepare the initial configurations of the i-PP melt comprising 120 chains (108,240 atoms). Four structures, with two sets of polymer chain configurations and two velocity seeds for each set, were simulated. Velocity-rescale thermostat (τ_T = 0.1 ps) and Berendsen[43] barostat (τ_P = 2.5 ps) were used in equilibration simulation to control the temperature and pressure, respectively, while Parrinello−Rahman[44] barostat (τ_P = 3.0 ps) was employed for property calculation trajectory. We equilibrated the system at 450 K which is well above the equilibrium melting temperature (396.4 K) of i-PP. Figure 1a shows the structure of the 120 i-PP chains after the execution of an equilibrium simulation.

Furthermore, the temperature was subsequently cooled to 180 K using various cooling rates. To find out the morphological properties of the i-PP melt system, a cubic box type was defined and we have minimized the structure to avoid any geometric inappropriateness. Furthermore, a NVT equilibration was performed to maintain the temperature of the system using velocity rescaling for 500 ps and a simulated annealing process took place during NPT equilibration of the melt system for 20 ns to achieve the local equilibrium by using Berendsen barostat. After making constant temperature and pressure of the system, MD production run was performed for 100 ns with a time step of 2 fs at a temperature of 450 K.

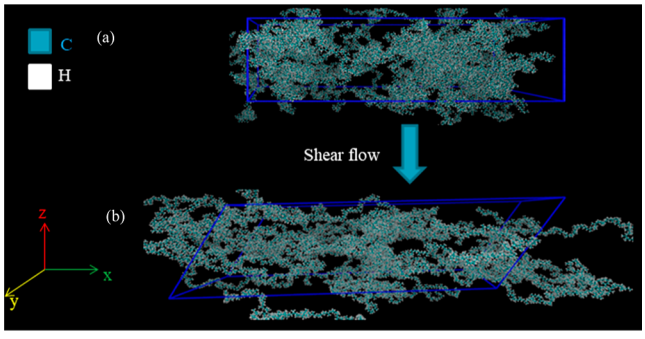

Figure 1. (a) Schematic representation of the i-PP polymer melt at equilibrium; (b) i-PP melt under shear.

2.2. Shear and Cooling Simulations. Followed by equilibration, a series of shear and cooling simulations were conducted to investigate the effect of shear flow and cooling rate on various properties of the i-PP melt. To ensure that system is in proper melt condition, the temperature was well above the melting point of i-PP. Semicrystalline polymers are extensively used in the polymer industry, and their crystallinity and morphology have a considerable effect on their mechanical and morphological characteristics. The morphology of these materials is influenced by several parameters, including the polymer's atomic structure, its thermal history, cooling rates, the presence of additives, and the melt's flow conditions during processing.[45]

To investigate the impact of shear rates, NEMD simulations were performed in the NPT ensemble. Four distinct well equilibrated initial structures from four sets of equilibrium simulations were simulated. Each system comprises 120 chains with an average box size of 20.172 nm × 7.748 nm × 7.307 nm along the x, y, and z directions, respectively. In order to minimize system size effects, we kept the box size sufficiently enlarged in the flow (x-) direction. We employed three distinct shear rates ($\dot{\gamma}_i$) of 2.62 × 10^8, 5.24 × 10^8, and 7.86 × 10^8 s^{-1} [corresponding to the highest value of Weissenberg no as 55.02, which is in the range of $W_i \in (1100)$] determined from the deform velocities of 0.002, 0.004, and 0.006 nm/ps, respectively (see Table 1).[46−48] Furthermore, the effect of cooling rates is explored by quenching the system after shear simulations. During the cooling process, the i-PP melt was cooled from 450 to 180 K by using different cooling rates ranging from 50 $\frac{\text{K}}{\text{ns}}$ (fast cooling), 5 $\frac{\text{K}}{\text{ns}}$ (medium cooling), and 1 $\frac{\text{K}}{\text{ns}}$ (slow cooling).[49]

2.2.1. Property Calculation. We computed the structural, dynamic, thermodynamic, and thermomechanical properties of i-PP by performing periodic annealing simulation, followed by a lengthy simulation (∼300 ns) coupled to V-rescale temperature at 450 K and Parrinello−Rahman barostat at 1 bar. Four repeat simulations were used to calculate all of the properties. The probability distributions for the radius of gyration and end-to-end distance of i-PP were determined from the trajectory of the last 50 ns. To investigate the dynamic response of i-PP, the self-diffusion coefficient of i-PP was calculated from the slope of the MSD plot. Some of the important properties calculated for the polymer system are described below.

2.2.2. Excess Entropy. To understand the ordered structure of the polymer solid, the two-body (pair correlation) contribution to conformational excess entropy, s_2, from the total RDF for polymer monomer−monomer beads, $G(r)$. Excess entropy is defined as the difference between the system thermodynamic entropy and that of an analogous ideal gas at particular temperature and pressure. The monomer−monomer RDF of i-PP was calculated to quantify its morphology and further used to calculate the two-body (pair correlation) contribution to excess entropy, s_2. The monomer−monomer

https://doi.org/10.1021/acsomega.3c03378
ACS Omega 2023, 8, 36775−36788

Table 1. Values of Shear Rates and Cooling Rates Considered during This Simulation Study

S.No	equilibrium simulation (no shear condition)	simulation 1 shear rate (γ) s^{-1}	simulation 2 shear rate (γ) s^{-1}	simulation 3 shear rate (γ) s^{-1}	cooling rate (fast) $\frac{K}{ns}$	cooling rate (medium) $\frac{K}{ns}$	cooling rate (slow) $\frac{K}{ns}$
1	0	2.62 × 108	5.24 × 108	7.86 × 108	50	5	1

(RDF), $g(r)$ was calculated for the center carbon which is attached to the functional group. An ensemble invariant expression for s_2 of a fluid at density ρ and temperature T is given by eq 1.[50]

$$s_{ex} \approx s_2 = -2\pi\rho\int_0^\infty [g(r)\ln g(r) - g(r) + 1]r^2 dr \quad (1)$$

To investigate the impact of shear flow on the morphology of i-PP, we have calculated the density, excess entropy, radius of gyration, end-to-end distance, and RDF of the polymer melt as well as frozen structures from equilibrated part of trajectory. In this paper, all the figures have been generated from the xmgrace plotting tool.

2.2.3. Elastic Moduli (E). Followed by shear and cooling processes, a series of uniaxial tensile simulations were conducted to determine the impact of shear rates and cooling rates on the tensile response of the i-PP polymer. Young's modulus (E_i) and Poisson ratio (v_{ji}) for the frozen structures were determined from a series of simulations in which strain was applied by stepwise uniaxial extension (+) or compression (−) along x, according to $x_n = (1 \pm n\epsilon_x)\, x_0$, where x_n is the box length along x in the nth simulation, x_0 = 20.172 nm is equilibrium length, and ϵ_x = 0.001. σ_{xx} component of stress tensor was used to calculate E_x. Furthermore, the Poisson ratio was calculated as ratio of strains perpendicular to applied stress and in the direction of applied stress, $v_{yx} = -\frac{\epsilon_{yy}}{\epsilon_{xx}}$. Similarly, E_y and v_{xy} were calculated from extension or compression along y.[51]

2.2.4. Glass Transition Temperature (T_g). Glass transition temperature, T_g, for i-PP was determined from specific volume-temperature (v−T) curves obtained from cooling simulations. Each of the (v−T) curves shows a slope change at some temperature, corresponding to the glass transition. The characteristic change in the slope of the (v−T) curve was used to calculate the T_g, as shown in Figure 9.[24] It is important to note that MD simulations typically use a very high cooling rate compared to experimental cooling rate. Therefore, T_g obtained from simulation does not correspond to the experimental value. To circumvent the issue of ultrafast cooling rates used in the simulation, WLF[52] equation was used to scale the T_g value obtained from simulation to the experimental cooling rates

$$\log a_t = \log \frac{\tau_{g,sim}}{\tau_{g,exp}} = \frac{-C_1(T_{g,sim} - T_{g,exp})}{C_2 + T_{g,sim} - T_{g,exp}} \quad (2)$$

where a_t is the shift factor and C_1 = 17.44, C_2 = 51.6 K are "universal" constants. $\tau_{g,sim}$ and $\tau_{g,exp}$ are the reciprocal cooling rates referring to $T_{g,sim}$ (simulated T_g) and $T_{g,sim}$ (experimental T_g), respectively.[27]

2.2.5. Polymer Viscosity. To investigate the viscous behavior of i-PP, we have used the periodic perturbation method in which an external force $a(z)$ is applied on the simulation box in the x-direction, and the shear viscosity is measured from the fluctuation of the induced momentum. Furthermore, we used Rosenfeld excess entropy scaling concept to establish the relationship which states that "A liquid obeys excess-entropy scaling if its reduced dynamic properties at different temperatures and pressures are determined exclusively by S_{ex}". Excess entropy scaling uses the so-called macroscopically reduced units, which vary with the thermodynamic state. Earlier, Voyiatzis et al. (2014)[53] have performed simulation and established a relationship between conformational excess entropy and reduced viscosity. In this work, we have used the correlation for reduced viscosity which is given as

$$\eta_R^* = \frac{\rho^{-2/3}}{\sqrt{mk_BT}}\eta \quad (3)$$

where ρ is the number density, m is the mass of monomer unit, k_B is the Boltzmann constant, and T is the temperature.[29,30,54]

3. RESULTS AND DISCUSSION

Below, we discuss results obtained for an extensive set of properties from equilibrium and nonequilibrium simulations. This section is divided into six different subsections: (3.1) structural properties, (3.2) thermodynamic properties, (3.3) dynamical properties, (3.4) mechanical properties, (3.5) physical properties, and (3.6) viscosity−entropy scaling. The outcomes of the first two sections were used to explain the observation of the last four sections. Shear simulations were carried out at a higher temperature (450 K) around 50 K above the melting point temperature. Furthermore, i-PP melt structures were cooled down and mechanical properties were calculated at 180 K around 80 K below T_g.

3.1. Structural Properties. Structural properties such as density, radius of gyration, end-to-end distance, and RDF were calculated from the equilibrium part of the long trajectory.

3.2. Density. To validate the simulation equilibration, the average density for i-PP that we found here is compared to that from the literature. The average densities of i-PP in melt, ρ_m, and solid state, ρ_s, obtained from the equilibrium simulations are 740.28 and 865 $\frac{kg}{m^3}$ at 450 and 180 K, respectively, as shown in Figure 2. These results are in close agreement with experimental measurements and simulation results on low molecular weight i-PP. The density of i-PP250 melt (measured by a specific gravity bottle) was reported to be 733 $\frac{kg}{m^3}$ at 523 K[55] and the density of PP42 melt (measured by a united atom simulation) was reported to be 730 $\frac{kg}{m^3}$ at 450 K.[56] Overall, these results show that the equilibrium density of the polymer melt was correctly determined and verify the validity of simulations.

Furthermore, we investigated the role of different shear flow and cooling rates on the density of i-PP. Figure 2a shows the density of i-PP at different shear rates at 450 K. After applying various shear rates on the order of 10^8 s^{-1} on i-PP at 450 K, we observed a slight decrease in the value of density. However,

https://doi.org/10.1021/acsomega.3c03378
ACS Omega 2023, 8, 36775−36788

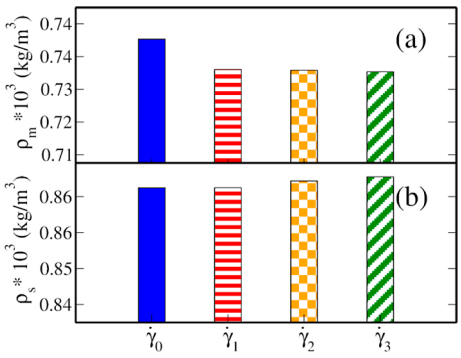

Figure 2. i-PP polymer density determined for equilibrium and nonequilibrium simulation at (a) 450 and (b) 180 K. Solid blue color indicates density at equilibrium (no shear), whereas red, orange, and green color represent density at shear rates of $\dot{\gamma}_1(2.62 \times 10^8\ s^{-1})$, $\dot{\gamma}_2(5.24 \times 10^8\ s^{-1})$, and $\dot{\gamma}_3(7.86 \times 10^8\ s^{-1})$ correspondingly.

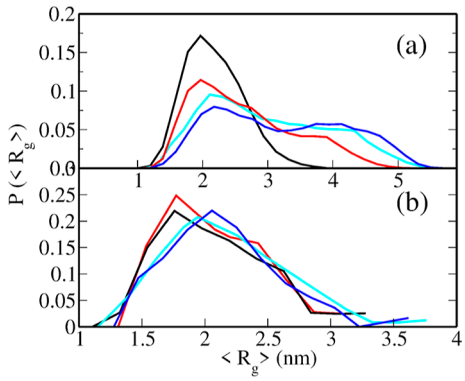

Figure 3. Probability distribution function of radius of gyration of i-PP polymer calculated at (a) 450 and (b) 180 K. The curve represented by solid black lines represents the case of equilibrium simulation $\dot{\gamma}_0$ (no shear), red, cyan, and blue lines represents R_g at the shear rates of $\dot{\gamma}_1(2.62 \times 10^8\ s^{-1})$, $\dot{\gamma}_2(5.24 \times 10^8\ s^{-1})$, and $\dot{\gamma}_3(7.86 \times 10^8\ s^{-1})$, respectively.

there was no significant effect on the density at three different shear rates as $\dot{\gamma}_1$, $\dot{\gamma}_2$, and $\dot{\gamma}_3$. At 450 K, the equilibrium density for a shear rate of $\dot{\gamma}_1$, $\dot{\gamma}_2$, and $\dot{\gamma}_3$ was found out to be 732.87, 732.68, and 732.3 $\frac{kg}{m^3}$, respectively, as shown in Figure 2a. Furthermore, we cooled down the melt structures, obtained from shear simulation, from 450 to 180 K. We employed fast cooling (1 $\frac{K}{ns}$) to quench the structures obtained after applying shear flow. Figure 2 shows that density of i-PP increases from 740.28 to 865 $\frac{kg}{m^3}$ on quenching the system. This observation qualitatively matches with the experimental work of Teh et al.[57] in which they reported the increases in density of polypropylene from 750 to 905 $\frac{kg}{m^3}$ as the system was cooled down from 485 to 298 K.[57] Here, the quenching process was also applied on all the systems (no shear and with shear). After cooling the system to 180 K at a cooling rate of 1 $\frac{K}{ns}$, densities of i-PP were found out to be 865.99, 867.51, and 868.4 $\frac{kg}{m^3}$ for aforementioned shear rates, as shown in Figure 2b. It was perceived that the density increases as we apply the shear flow rates, followed by slow cooling.

Additionally, we investigated the role of the cooling rate on polymer morphology. We change the rate of cooling from 1 to 50 $\frac{K}{ns}$. It is observed that the density of i-PP decreases as we increase the cooling rate. It is because the polymer gets less time to form an ordered structure.

3.2.1. Radius of Gyration of i-PP. To account for a second measure of the structure property of the i-PP melt, the dimensions of the polymer chains are calculated by quantifying the value of radius of gyration, which is denoted by a symbol "R_g". It is represented by probability distribution curve for the last 50 ns and represented, as shown in Figure 3. From Figure 3a, the average value of R_g for i-PP melt at 450 K is obtained as 2.09 nm which matches excellently with the experimental work of Ballard et al.[58] calculated by using small-angle neutron scattering studies and from the simulation work of Khan and Goel,[51] by using the Martini-coarse grain model at 450 K in which they have reported the value of R_g as 1.95 nm at 450 K. In 2019, Tsamopoulos et al.[59] performed NEMD simulation of poly(ethylene oxide) to study the shear rheology between ring and linear polymer melt. They examined the impact of shear rates on conformational properties and concluded that the radius of gyration increases in the direction of shear on increasing the shear rate.

In this work, it is evident from Figure 3a that as we apply the shear rates, the peak of the curve gets shifted to the right side as well as the increase in the second peak which represents an increase in the value of R_g. At 450 K, R_g of i-PP was calculated as 1.96 nm under equilibrium condition, while it gets increased from 2.01 nm, 2.13 to 2.23 nm after applying the shear rates of $\dot{\gamma}_1(2.62 \times 10^8\ s^{-1})$, $\dot{\gamma}_2(5.24 \times 10^8\ s^{-1})$, and $\dot{\gamma}_3(7.86 \times 10^8\ s^{-1})$. This is due to the shear field deforming the arrangement of the molecules and lengthening the chain as the shear rate increases. Moreover, it is also clear from the Figure 3b that as we cool down the structure obtained from no shear simulation from 450 to 180 K, the atoms come closer to each other which ultimately results in decrease in the value of R_g from 1.96 to 1.56 nm at equilibrium. However, in the case of NEMD simulation, the value of radius of gyration (R_g) decreases to 1.58, 1.95, and 2.1 nm, respectively, at a particular cooling rate of 1 $\frac{K}{ns}$. This result validates with the simulation work of Yamamoto et al., in which they cooled down the system of i-PP from 700 to 200 K by applying stepwise cooling and they have observed the drop in the value of R_g after cooling at a rate of 10 $\frac{K}{ns}$.[60]

Additionally, we have cooled the i-PP melt from 450 to 180 K by applying different cooling rates to understand the change in the conformational characteristics of the polymer. To look at the impact of the cooling rate on R_g under equilibrium conditions, we have applied various cooling rates from 1 to 50 $\frac{K}{ns}$. It is observed that as we increase the cooling rate, the value of R_g increases and it was found out to be 1.76, 1.95, and 2.22 nm at a cooling rate of 1, 5, and 50$\frac{K}{ns}$, respectively. It is obvious from the result that this simulation study quantitatively validates the experimental and simulation work reported in literature.

3.2.2. End-to-End Distance. Another structural property that defines the chain dimension of a polymer is the end-to-end distance (R_e). For each molecule, R_e is computed by utilizing the first and final atoms in the index group, and its value is calculated to quantify the morphology of the polymer melt. In this simulation study, the average value of R_e of i-PP melt at 450 K is calculated for the last 50 ns and it was found

https://doi.org/10.1021/acsomega.3c03378
ACS Omega 2023, 8, 36775−36788

to be 4.04 nm at equilibrium conditions, which matches very well with the simulation study of Heine et al., which reported the value of R_e as 3.46 nm by using LAMMPS force field for i-PP24 of chain at 453 K and also from the simulation work of Khan and Goel, calculated by using MARTINI coarse grain model at 450 K for i-PP.[51,61]

Furthermore, we also performed NEMD simulations to find out the effect of shear and cooling rates on the conformational changes of i-PP during melt conditions as well as after quenching. It is obvious from Figure 4a that as we apply the

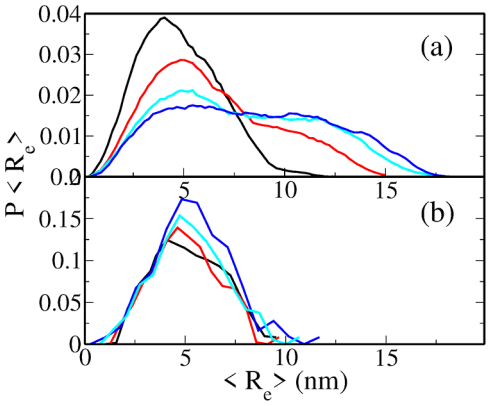

Figure 4. Probability distribution function representing the R_e of i-PP polymer calculated at (a) 450 and (b) 180 K. The curve represented by solid black lines represents the case of equilibrium simulation, red, cyan, and blue lines represents R_e at the shear rates of 2.62×10^8 s^{-1}, $\dot{\gamma}_2(5.24 \times 10^8$ $s^{-1})$, and 7.86×10^8 s^{-1}, respectively.

shear rates, the peak of the curve gets shifted to the right side which shows an increase in the value of R_e. At 450 K, the value of R_e for i-PP increases to 5.06, 5.18, and 5.49 nm after applying the shear rates of 2.62×10^8, 5.24×108, and 7.86×10^8 s^{-1}, respectively. Moreover, it is also clear from Figure 4b that as we cool down the simulation system from 450 to 180 K, the atoms come closer to each other, which ultimately results in the decrease in the value of R_e from 4.2 to 4.08 nm at equilibrium. However, in the case of NEMD simulation, the value of end-to-end distance (R_e) decreases to 4.6 and 5.06 nm, respectively, at a cooling rate of 1 $\frac{K}{ns}$. Guan et al. have performed MD simulation to study the structural, kinetic, and thermodynamic behavior of PP3000 during heating and cooling process. During the cooling, it was observed that the peak of the probability distribution curve shifts to the left side which indicates the decrease in the R_e of PP3000 due to the enwinding of the polymer chain after cooling.[13] From the above-mentioned result, it is clear that the value of the end-to-end distance of i-PP calculated in the current simulation study qualitatively validates with the reported simulation work.

3.2.3. Radial Distribution Function. The RDF is commonly used to determine how atoms assemble around one another. Because it is dependent on the density and temperature, it is a valuable indicator of the nature of the phase taken by the simulated system in MD. Calculating the RDF is necessary to comprehend the influence of cooling and shear flow on a polymer's structural property. In this paper, we have calculated the monomer−monomer RDF of i-PP around the center carbon that is attached to the functional group. In Figure 5, we have plotted the RDF plot for 450 and 180 K. We observed a small difference in the peaks of monomer−monomer RDFs at

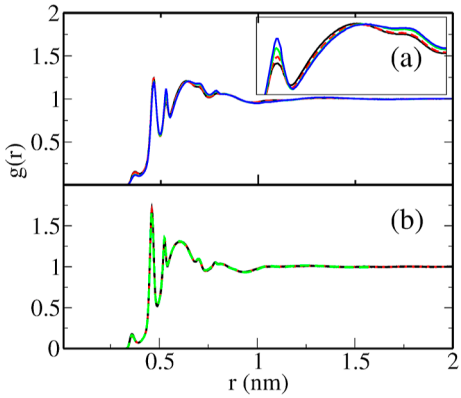

Figure 5. RDF plot of the i-PP polymer calculated at 450 K. (a) The curve represented by solid black lines represents the case of equilibrium simulation, while red, green, and blue lines represents R_e at the shear rates of 2.62×10^8, 5.24×108, and 7.86×10^8 s^{-1}, respectively, and at 180 K. (b) The curve represented by solid black lines represents the case of equilibrium simulation, while red and green lines represents R_e at the shear rates of 2.62×10^8 and 7.86×10^8 s^{-1}, respectively.

450 K as shown in Figure 5a, with the key difference being a small increase in second and successive peaks on increasing the shear rates. This indicates that higher shear rate increases the ordering and in turn more crystalline structure of the i-PP polymer. However, at the low temperature (450 K) after cooling with, 1 $\frac{K}{ns}$, we have observed that there were no significant changes, and the curve overlaps each other for i-PP under equilibrium as well as nonequilibrium conditions, as shown in Figure 5b. This behavior matches well with the simulation study of Nagarajan and Myerson in which they have performed the molecular simulation with four i-PP chain (containing 90 backbone carbon) with and without a nucleating agent.[62] Furthermore, we have also examined the impact of cooling rates (1, 5 and 50 $\frac{K}{ns}$) for i-PP for equilibrium simulation, which is shown in Figure 6. We observed that RDF peaks slightly decrease as we increase the cooling rates. This shows fast cooling suppresses the formation of the crystal structure.

3.3. Thermodynamic Property. Notably, it was shown that interpretation made on dynamical properties, using model

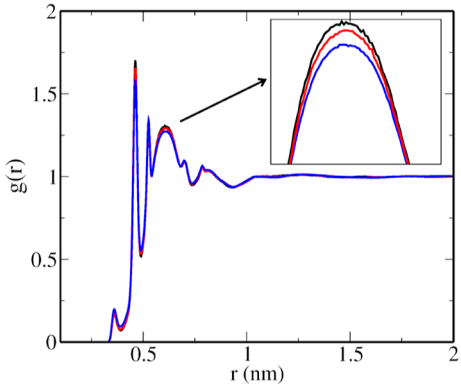

Figure 6. Comparison of rdf at equilibrium conditions for different cooling rates. Black color line represents the cooling rate of 1 $\frac{K}{ns}$, red color line represents 5 $\frac{K}{ns}$, and blue color line represents 50 $\frac{K}{ns}$.

https://doi.org/10.1021/acsomega.3c03378
ACS Omega 2023, 8, 36775−36788

wall colloid interactions, based on extent of particle layering can be ambiguous and conformational excess entropy was instead used to elucidate the relationship between diffusion of colloidal particles and wall colloid interaction.[63] Therefore, the two-body contribution to excess entropy, s_2, a thermodynamic property, was calculated from monomer−monomer RDFs. The thermodynamic property of polymer is an integrated part of characterization of material science. To gain insights into the thermodynamic property, excess entropy (s_2) of i-PP polymer was calculated from the time-dependent RDF data as shown in eq 1. It was observed that at 450 K, the excess entropy decreases after applying a shear rate of $\dot{\gamma}_1(2.62 \times 10^8\ s^{-1})$, $\dot{\gamma}_2(5.24 \times 10^8\ s^{-1})$, and $\dot{\gamma}_3(7.86 \times 10^8\ s^{-1})$, as compared to i-PP melt at equilibrium as shown in Figure 7a. This is due to the

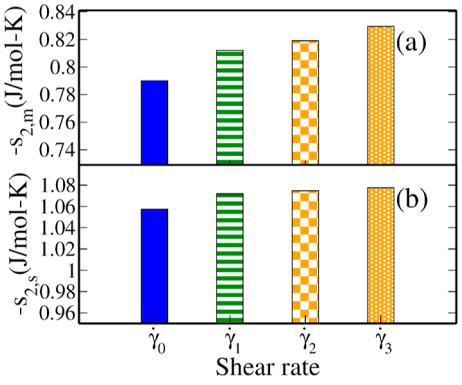

Figure 7. Bar representation on the effect of shear rates on the excess entropy of i-PP polymer calculated at (a) 450 and (b) 180 K. The bar represented by solid blue color represents the case of equilibrium simulation $\dot{\gamma}_0$ (no shear), green, yellow, and orange color bar represents excess entropy at the shear rates of $\dot{\gamma}_1(2.62 \times 10^8\ s^{-1})$, $\dot{\gamma}_2(5.24 \times 10^8\ s^{-1})$, and $\dot{\gamma}_3(7.86 \times 10^8\ s^{-1})$, respectively.

chain relaxation at higher shear rates, which causes the simulation system to become more ordered. At 450 K, the excess entropy was determined for equilibrium as well as NEMD simulation and it was reported as $-0.79518\ \frac{J}{mol\text{-}K}$ at equilibrium while −0.81109, −0.81785, and $-0.82885\ \frac{J}{mol\text{-}K}$ at aforementioned shear rate.

After cooling down i-PP melt from 450 to 180 K at a particular cooling rate of $1\ \frac{K}{ns}$, it was observed that there was a decrease in the excess entropy as the molecules gets ordered after cooling. At equilibrium, the excess entropy was calculated as $-1.05736\ \frac{J}{mol\text{-}K}$ at 180 K, while at a shear rates of $\dot{\gamma}_1(2.62 \times 10^8\ s^{-1})$, $\dot{\gamma}_2(5.24 \times 10^8\ s^{-1})$, and $\dot{\gamma}_3(7.86 \times 10^8\ s^{-1})$, it was found out to be −1.07196, −1.07469, and $-1.07742\ \frac{J}{mol\text{-}K}$, respectively, as shown in Figure 7b. To further investigate the effect of cooling rates, we have calculated the excess entropy of i-PP at equilibrium, and we have observed that as we increase the cooling rates from 1 to $50\ \frac{K}{ns}$, the excess entropy increases which indicates that the system gets disordered as the cooling rates increases. At equilibrium condition, the excess entropy was reported as −1.05736, −1.045, and $-0.97082\ \frac{J}{mol\text{-}K}$ after cooling down at the rate of 1, 5, and $50\frac{K}{ns}$, respectively. Finally, we note that for all cases, there is a small change in local ordering as observed in RDFs which is clearly manifested by increase or decrease in $|s_2|$ values.

3.4. Dynamical Property. Diffusion coefficient is the most important analytical parameter used in determining the dynamics of polymers. To fully understand the dynamic behavior of polypropylene melt, the self-diffusion coefficient is calculated by using an Einstein diffusion equation for a long time slope of MSD curve.[51] In this work, the value of self-diffusion coefficient of i-PP melt of molecular weight 4200 g/mol is calculated to be $9.38 \times 10^{-7}\ \frac{cm^2}{s}$ from the slope of MSD curve and it matches very well with the experimental study of von Meerwall, et al. They have determined by using pulse-grained diffusion experiment and nuclear magnetic resonance technique for linear i-PP melts of molecular weight $9900\ \frac{g}{mol}$ and the value obtained was $2.7 \times 10^{-8}\ \frac{cm^2}{s}$ at 453 K.[16]

3.5. Mechanical Property. The Young's modulus (E) one of the important mechanical properties of a material was determined from the slope of the stress−strain curve at 180 K, much below the glass transition temperature, which refers to a material's first response to strain and is ascribed to the material's stiffness at deformation. E is determined from the component of the stress tensor calculated in the limit of slow uniaxial extension or compression. We obtained E of 2.3 GPa at 180 K from equilibrium simulation (no shear) which is in good agreement with the experimental value reported by Glüge[64] (1.53 GPa with crystallinity of 30−35%), and from the experimental work of Phulkerd et al. in which they have observed that Young's modulus of PP with a nucleating agent (i.e., *N,N′*-dicyclohexyl-2,6-naphthalene dicarboxamide) is 766 MPa which is larger as compared to a pure PP of Young's modulus (628 MPa) in the machine direction using a T-die extrusion. Young's modulus value obtained in our simulation is also in good agreement with value reported by Qian and Ludovice, in which they have obtained the modulus as 0.9 GPa, calculated by using CHARMM force field at 250 K for i-PP.[18,65]

To determine the effect of shear flow on the thermomechanical properties of i-PP, three shear rates as $\dot{\gamma}_1(2.62 \times 10^8\ s^{-1})$, $\dot{\gamma}_2(5.24 \times 10^8\ s^{-1})$, and $\dot{\gamma}_3(7.86 \times 10^8\ s^{-1})$ were employed in NEMD simulation at 450 K. Final structures obtained from theses simulations were cooled down to 180 K by a cooling rate of $1\ \frac{K}{ns}$. Figure 8a shows that the Young's modulus increases with an increase in the value of the shear rate. We obtained Young's modulus of 2.317, 2.33, and 2.35 GPa at shear rates $\dot{\gamma}_1$, $\dot{\gamma}_2$, and $\dot{\gamma}_3$, respectively. This trend of an increase in the Young's modulus of i-PP is in good agreement with trends observed in experiments.[34,35] Using frequency sweep experiment, Koscher and Fulchiron demonstrated that the Young's modulus of PP rises with the increase in shear rate.[34] Although the rise in Young's modulus is minimal, the excess entropy showed the same trend. Therefore, this enhancement can be attributed to the formation ordered structure as represented by the decrease in excess entropy with the increase in shear rates.

To investigate the effect of cooling rate, the i-PP melt structure obtained after equilibrium simulation (no shear) was cooled down to 180 K by applying three cooling rates (1, 5, and $50\ \frac{K}{ns}$). In line with the general experimental trend of fast cooling decreasing the elastic moduli of polymer,[66] we observed a decrease in the elastic modulus from approximately

https://doi.org/10.1021/acsomega.3c03378
ACS Omega 2023, 8, 36775−36788

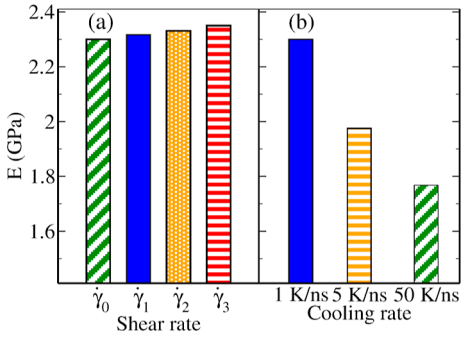

Figure 8. (a) After applying three different shear rates, the Young's modulus of i-PP for equilibrium and nonequilibrium simulation (NEMD) at a specific cooling rate of 1 K/ns was computed at 180 K. Young's modulus shown by a green color bar is for equilibrium simulation (2.3 GPa), whereas blue color solid bar (2.317 GPa), an orange color bar (2.33 GPa), and a red color bar (2.35 GPa) for the Young's modulus after applying the shear rates of $\dot{\gamma}_1(2.62 \times 10^8\ s^{-1})$, $\dot{\gamma}_2(5.24 \times 10^8\ s^{-1})$, and $\dot{\gamma}_3(7.86 \times 10^8\ s^{-1})$, respectively. (b) The i-PP Young's modulus under equilibrium conditions with various cooling rates. The Young's modulus is represented by the color bars in blue (2.3 GPa), orange (1.97 GPa), and green (1.76 GPa) at cooling rates of 1, 5, and 50 K/ns, respectively.

2.3 GPa for slow cooling to 1.76 GPa for fast cooling, as shown in Figure 8b. These results showed that slow cooling rate is favorable to enhance the Young's modulus due to an increase in the crystalline content in the polymer as observed in experiments.[66] However, Hassani et al. have experimentally measured the impact of cooling rate on the mechanical property of polypropylene self-reinforced composites. They have visualized a decrease and then increase in the value of modulus with an increment in the cooling rate from 2.5 to 40 °C/min.[67] Our simulations reveal that the high shear rate and slow cooling increase the Young's modulus of i-PP significantly. This enhancement mechanism depends on the formation of an ordered or crystal structure in the polymer caused by slow cooling and high shear flow. It was reported that an increase in α-crystalline phase content promotes the increase of specific oriented morphology, which makes the i-PP more rigid and causes an increase in Young's modulus.[21] However, due to the sluggish nature of crystallization and ultrafast cooling rates used in this study, we have calculated a thermodynamic property, i.e., excess entropy instead of determining the crystallization here. To understand the variation in mechanical property, we have correlated the change in excess entropy with the change in Young's modulus. We observed 23.02% change in the value of E as we increase the cooling rate from 1 to 50 K/ns. Similar change in excess entropy (8.18%) was observed at the same cooling rates. The decrease in the excess entropy indicates the formation of an ordered structure at a slow cooling rate. Slow cooling offers polymers more time to relax and create ordered or crystalline structures, which increases the Young's modulus.

3.6. Physical Properties. *3.6.1. Glass Transition Temperature (T_g).* We used specific volume−temperature ($v-T$) curve to calculate the glass transition temperature (T_g), the transition temperature between glassy and rubbery state of polymer.[68−70] The $v-T$ curve was generated using data obtained from cooling simulations performed under the *NPT* ensemble. Three cooling rates of 1, 5, and $50\frac{K}{ns}$ were used to cool down the system from 450 to 180 K. According to the free volume theory, the specific volume changes linearly with temperature but has distinct slopes below and above the glass transition point.[23,24,71] The intersection of the two linear fitted curves at both ends of the volume-temperature curve gives the T_g of i-PP. Figure 9 shows the fitted curves of specific volume versus

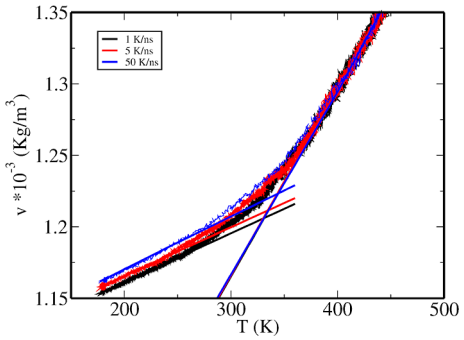

Figure 9. Specific volume vs temperature curves for i-PP after applying three different cooling rates of 1, 5, and 50 K/ns are plotted. The slopes represented by the black color line intersect to produce the reported glass transition temperature of 331 K at 1 K/ns. Similarly, the intersection of red lines produces a glass transition temperature of 338 K at 5 K/ns.

temperature for i-PP calculated at different cooling rates for the system obtained from no shear simulation. We obtained values of T_g in the range of 330 to 350 K which are in good agreement with the results obtained by Yu et al., who determined T_g (364 K) for bulk and freestanding thin films of atactic polypropylene from MD simulation using Dreiding II force-field.[24] Since T_g values obtained in our simulation as well as in other MD simulation studies are substantially higher than those reported in experiments (the experimental value 253−262 K).[72,73] The difference between T_g values obtained from simulations and experiments is considered to be the consequence of the ultrahigh cooling rate (1 to 50 K/ns), which was much faster than that used in experiments. Therefore, to circumvent the problem arises due to the use of fast cooling used in MD simulations, we utilized the Williams−Landel−Ferry (WLF) equation to shift the simulated T_g value to the corresponding experimental cooling rates. We obtained the shifted T_g values in a range of 269.02 K that are much closer to the experimental values of i-PP.

T_g reveals the rate of rearrangement of molecules in supercooled liquid, and it is a crucial indicator to measure the thermal characteristic of polymers among the many transitions and relaxations. In i-PP polymer, shear-induced conformational changes and cooling rates are crucial factors in defining attributes such as the T_g. Therefore, in this work, we investigated the thermodynamics of variation in T_g due to applied shear flow and cooling rate. In various studies, it is proposed that the variation in mechanical and physical properties observed due to the formation of crystal or ordered structure. Due to the fast cooling used in simulation and considering the sluggish nature of crystallization in i-PP, we utilized the thermodynamic property s_2 to explain the variation in T_g.

We investigated the impact of the shear rate on the glass transition temperature. The given Figure 10a illustrates the plot of shifted glass transition temperatures obtained from cooling simulations of the structures obtained from no shear as well as shear simulations. A cooling rate of $1\frac{K}{ns}$ was used to

https://doi.org/10.1021/acsomega.3c03378
ACS Omega 2023, 8, 36775−36788

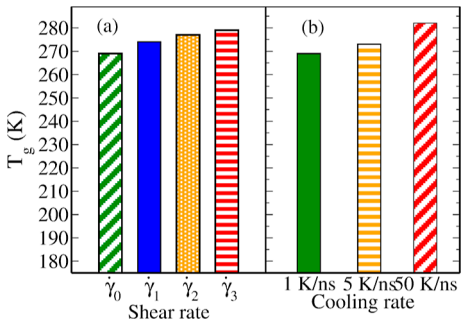

Figure 10. (a) Changes in the glass transition temperature of i-PP at a specific cooling rate of 1 K/ns for equilibrium and nonequilibrium simulations (NEMD). Green color bar indicates T_g for equilibrium simulation (269.02 K), while blue color bar (268.02 K), orange color bar (267.81 K), and red color bar (267.23 K) reflect the T_g for shear rates of $\dot{\gamma}_1(2.62 \times 10^8\ s^{-1})$, $\dot{\gamma}_2(5.24 \times 10^8\ s^{-1})$, and $\dot{\gamma}_3(7.86 \times 10^8\ s^{-1})$, respectively. (b) Variation of the shifted glass transition temperature for the i-PP equilibrium simulation under various cooling rates. T_g after cooling down at rates of 1, 5, and 50 K/ns is represented by the color bars in green (269.02 K), orange (273.03 K), and red (282.05 K), respectively.

cool down all the structures. It is shown that T_g slightly decreases by applying a shear rate of $\dot{\gamma}_1(2.62 \times 10^8\ s^{-1})$, $\dot{\gamma}_2(5.24 \times 10^8\ s^{-1})$, and $\dot{\gamma}_3(7.86 \times 10^8\ s^{-1})$, respectively. The decrease in T_g can be attributed to the reduction in the free volume as high shear promotes dense structure due to the formation of a more ordered structure. This can be further validated in the decrease in the excess entropy. We observed 1.82% change in the value of T_g as we increase the shear rate from 2.62×10^8 to $7.86 \times 10^8\ s^{-1}$. Similar change in excess entropy (1.8%) was observed at the same shear rates. This shows that the system becomes more ordered as we increase the shear rate, and due to this more ordered structure, crystal content will increase, while amorphous content will decrease. Therefore, it can be concluded that the decrease in the T_g with an increase in shear rates is due to the decrease in the amorphous or less ordered content.

Furthermore, we investigated the effect of cooling rates on T_g. Polymer melt structures obtained from shear and no shear simulation were cooled down from 450 to 180 K by applying three different cooling rates of $1\ \frac{K}{ns}$ (very slow cooling), $5\ \frac{K}{ns}$ (slow cooling), and $50\ \frac{K}{ns}$ (fast cooling). Figure 10b represents that as we increase the cooling rate from 1 to $50\ \frac{K}{ns}$, the glass transition temperature increases from 269.02 K $\left(1\ \frac{K}{ns}\right)$ to 282.05 K $\left(50\ \frac{K}{ns}\right)$. Here, we observed a qualitative trend in increase in T_g on increasing the cooling rate as observed in experimental studies.[74−76] However, this observation contradicts with the observation from the experimental work of Schawe in which he showed the decrease in T_g of polypropylene on increasing cooling rate from 1 to 4000 $\frac{K}{s}$ while studying crystallization phenomenon in i-PP using differential scanning calorimetry.[25,77,78] In our previous work, we also observed a decrease in the T_g with an increase in the cooling rate. This error might be due to the use of only one structure for T_g calculation and the use of the same experimental cooling rate to scale the simulated T_g. In this work, we used the average T_g obtained from the cooling of four distinct structures at a particular cooling rate. Furthermore, while using the WLF equation to scale the simulated T_g, we kept the ratio of experimental and simulation cooling rate same.

The increase in glass transition temperature can be correlated with the increase in excess entropy on an increasing cooling rate. We observed 4.82% change in the value of T_g as we increase the cooling rate from 1 to 50 K/ns. Similar change in excess entropy (8.18%) observed at same cooling rates. However, even though T_g increased, the excess entropy of the polymer increased, indicating a loose or less ordered packing. These two concepts of long-range mobility and less ordered packing are difficult to combine into a single theory. We anticipate that it is because of partial crystallization during the cooling process. The slower cooling rate will allow more crystallization or more ordering, and therefore, amorphous content will reduce, which leads to the decrease in T_g.

It was observed that polymers did not crystallize if fast cooling was used. Experimental studies revealed that during slow cooling rate, α-crystalline lamellae form is observed whereas at fast cooling, mesophase aggregates formed. The structure of the mesomorphic phase is less ordered compared to the long-range ordered structure observed in α-phase lamellae. Fast cooling suppressed the long-range ordering that is required for crystallization. However, we observed a change in thermodynamic, mechanical, and physical properties of the polymer during fast cooling. Therefore, we correlate the variation in mechanical properties and glass transition temperature with the changes in excess entropy. Here, entropy changed due to some structural changes or local ordering. We conclude that shear and cooling induced ordering of polymer monomers/molecules leads to changes in mechanical and physical properties.

3.6.2. Shear Viscosity. Shear viscosity is critical for maintaining stable processing conditions and delivering the desired product characteristics. In various studies, it is reported that the viscosity of a polymer melt is affected by shear rate, temperature, pressure, molecular structure, and fabrication conditions. In this work, we investigated the effect of the shear rate on melt viscosity. Shear rate is important because it may influence viscosity, which impacts the process ability and application of various materials.[79,80] One of the primary characteristics for a polymeric material is non-Newtonian behavior, which exhibits a decrease in the viscosity of the polymer melt as the shear rate increases. During processing, the shear force reorganizes the random polymer chains into an aligned conformation that reduces melt viscosity during the process.[81] However, the effect of shear thinning varies among polymers with a high molecular weight. Understanding of this behavior is crucial for processing, as it enables easy dispensing of the melt when pressure is applied.

These factors influence the rheological behavior or, to be specific, the melt viscosity of iPP. If the viscosity of molten PP is not suitable within the processing conditions, short shot or flashing may occur in injection molding. These problems are essentially crucial to be addressed since the modification of thermoplastic viscosity will also modify the end properties of the produced product. With regard to its flow behavior, a better understanding of PP rheological characteristic can overcome the existing difficulties and literally secure a successful processing. Additionally, viscosity in melted plastics is influenced by factors like temperature, molecular weight distribution, and chain branching, impacting the material's flow behavior.[82,83] To investigate the viscous behavior of i-PP, we

https://doi.org/10.1021/acsomega.3c03378
ACS Omega 2023, 8, 36775−36788

have used the periodic perturbation method in which an external force $a(z)$ is applied on the simulation box in the x-direction and the shear viscosity is measured from the fluctuation of the induced momentum. We have observed that polymer melt showed shear-thinning behavior of viscosity; i.e., as we increase the shear rate, the shear viscosity decreases. This behavior is validated by the experimental work of Meng et al. in which they have investigated the rheological behavior of polypropylene in a capillary flow, and they have concluded that the shear viscosity decreases significantly with an increase in the shear rate of the order of 4×10^2 to 10^4 s^{-1}.[84]

3.7. Reduced Viscosity−Entropy Scaling. Currently, the excess entropy has been calculated using complex measurements of the microstructure, which can be inconvenient and difficult to obtain. It would be advantageous to find an equation that relates the excess entropy to more readily measurable quantities like shear induced diffusivity, shear viscosity, etc.[85] The above sections show a consistent effect of shear and cooling rate on polymer chain structure (R_g, R_e), polymer morphology (density, RDF), chain diffusion coefficient, glass transition temperature, viscosity, and elastic properties. The viscous behavior of polymer melt under steady shear condition can be further quantified by Rosenfeld excess entropy−viscosity scaling which is applicable for a variety of complex fluids.[29,30] Although excess entropy is considered as an equilibrium thermodynamic quantity, Krekelberg et al.[86,87] proposed using the two-body excess entropy s_2 (two body contribution to excess entropy) calculated from eq 1 in order to extend excess-entropy scaling to out−of equilibrium situations. This approach has been used for diverse set of systems to collapse relaxation time data.[88] With the results of shear viscosity and rdf calculated from MD simulation, we used the Rosenfeld excess entropy−viscosity relationship to compare and contrast the polymer behavior under different shear rates. We calculated monomer beads' excess entropy by only considering the center carbon which is attached to the functional group. In Figure 11, reduced viscosity and excess entropies of i-PP polymer melt at different shear rates are plotted.

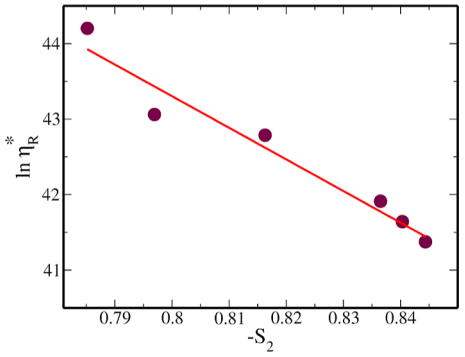

Figure 11. Variation in reduced effective viscosity, η_R^*, plotted vs two-body contribution to excess entropy of i-PP calculated at 450 K.

We observed an exponential relationship of s_2 with reduced viscosity of polymer. Rosenfeld demonstrated that the reduced viscosity is correlated to the excess entropy in a quasi-universal by $\eta_R^* = 0.033\ e^{-1.57 s_2}$, while we observed scaling law for reduced viscosity as $\eta_R^* = 29.12\ e^{-41.91 s_2}$ for the i-PP melt. A similar exponential relationship for viscosity-excess entropy has been obtained for a various set of systems.[86,89] As discussed earlier, an increase in shear flow organized/aligned the randomly oriented polymer chains that leads to the decrease in shear viscosity, and this behavior is well captured by Rosenfeld's excess entropy scaling. This provides insights into the dependency of viscosity on the structure and thermodynamics of the polymeric melt.

4. CONCLUSIONS

In this work, we discuss the thermodynamic insights into variation in mechanical and physical properties of i-PP polymers under processing conditions such as shear flow and cooling rates. NEMD simulations were used to understand how shear flow and cooling rates affect the ordering at molecular level and overall chain conformation. To this end, we have calculated an excess entropy, a thermodynamic property from monomer−monomer RDFs to elucidate the effect of shear flow and cooling process on various properties of polymeric materials. The equilibration of the simulation was tested, and the radius of gyration and end-to-end distance of i-PP were calculated to understand its morphological aspect at the microscopic level. The simulation results are perfectly in line with the experimental data. The density, the radius of gyration, and end-to-end distance of i-PP changed with shear rate. The density of the i-PP melt decreased with the increase in the shear rates, while the radius of gyration and end-to-end distance of polymer chains increased with increment in shear rates. As the shear rate was increased, it was also noticed that the Young's modulus increased while the glass transition temperature decreased. The shear flow reduces the free energy gap and improves conformational ordering, which helps to produce crystalline polypropylene. Excess entropies were calculated in all cases. On increasing shear rate results in excess entropy decreased, which indicates that the system becomes more ordered. As a result, the rise in shear rate which accelerates the formation of ordered structure may be associated with a consequent drop in glass transition temperature and excess entropy.

Furthermore, the polymer becomes denser with a decrease in the cooling rate because of the improved ordered or crystal structure. With an increase in the cooling rate, excess entropy increases, indicating that polymer has less time to get an ordered structure. On increasing the cooling rate, Young's modulus declines because of the rise in excess entropy; however, the glass transition temperature rises. Due to the sluggish crystallization process in i-PP, typically no crystal phase formed in the fast-cooling process. Fast cooling significantly suppressed the long-range ordering that is required for crystallization. Therefore, we did not specifically look for crystallization in this study. We correlate the variation in mechanical properties and glass transition properties with the changes in excess entropy.

At slow cooling, the excess entropy decreases, while Young's modulus increases, which implies that the more ordered structure promotes the rigidness in polymer. Furthermore, the study on viscous behavior of the i-PP melt with different shear rates indicated the shear-thinning behavior of the polymer melt. We relate this shear thinning behavior of i-PP to the associated structural rearrangement of the polymer under shear flow. Moreover, we have quantified this connection using viscosity-excess entropy scaling, where the latter captures static and higher order correlations between monomer positions. Rosenfeld excess entropy scaling showed a linear relationship between the reduced viscosity and excess entropy. Overall, the

https://doi.org/10.1021/acsomega.3c03378
ACS Omega 2023, 8, 36775−36788

present work explains the link between mechanical, physical, and thermodynamic properties.

AUTHOR INFORMATION

Corresponding Authors

Parvez Khan − *Department of Chemical Engineering, Aligarh Muslim University, Aligarh 202002, India*; orcid.org/0000-0003-0865-145X; Email: pkhan@myamu.ac.in

Naseem A. Khan − *Department of Chemical Engineering, Aligarh Muslim University, Aligarh 202002, India*; Email: nakhan@zhcet.ac.in

Authors

Ahmad S. Jawed − *Department of Chemical Engineering, Aligarh Muslim University, Aligarh 202002, India*

Mohd Nasir Khan − *Department of Chemical Engineering, Aligarh Muslim University, Aligarh 202002, India*

Mohammed A. Hakeem − *Department of Chemical Engineering, Aligarh Muslim University, Aligarh 202002, India*

Complete contact information is available at: https://pubs.acs.org/10.1021/acsomega.3c03378

Author Contributions

A.S.J. and M.N.K. have made an equal contribution. Main idea and outline of the manuscript was conceived by PK. All the authors contributed to the writing of the manuscript. The final version of the manuscript has approved by all authors.

Notes

The authors declare no competing financial interest.

ACKNOWLEDGMENTS

The authors are thankful to the department of Chemical Engineering, AMU Aligarh for arranging the facility for computational resources.

REFERENCES

(1) D.Ferry, J. *Viscoelastic Properties of Polymers*; John Wiley & Sons, Ltd., 1980.

(2) Pokharel, P.; Wei, F.; Shi, J.; Wang, Y.; Xiao, D. Thermomechanical properties of polypropylene and styrene-ethylene-butylene-styrene blends: a molecular simulation and experimental study. **2021**, arXiv:2101.03426.

(3) Larson, R. G. *The structure and rheology of complex fluids-RG Larson.pdf*; Oxford University Press, 1999.

(4) Bird, R. B.; Armstrong, R. C.; Hassager, O. Dynamics of polymeric liquids - Vol. 1: Fluid Mechanics, 2. Ausgabe. 649 Seiten, Preis: £64.15. *Ber. Bunsenges. Phys. Chem.* **1987**, *91*, 1397.

(5) Maddah, H. A. Polypropylene as a Promising Plastic: A Review. *Am. J. Polym. Sci.* **2016**, *6*, 1.

(6) Yang, L.; Zhang, L.; Webster, T. J. Nanobiomaterials: State of the Art and Future Trends. *Adv. Eng. Mater.* **2011**, *13*, B197−B217.

(7) Seki, M.; Thurman, D. W.; Oberhauser, J. P.; Kornfield, J. A. Shear-mediated crystallization of isotactic polypropylene: The role of long chain-long chain overlap. *Polym. Prepr. (Am. Chem. Soc., Div. Polym. Chem.)* **2002**, *35*, 2583−2594.

(8) Maia, J.; Covas, J.; Gabriele, D. Rheology in Materials Engineering. *Rheology*; Eolss Publishers Company Limited, 2010; Vol 2.

(9) Liang, J. Z.; Li, R. K. Y. Rubber toughening in polypropylene: A review. *J. Appl. Polym. Sci.* **2000**, *77*, 409−417.

(10) Naffakh, M.; Marco, C.; Ellis, G. Novel polypropylene/inorganic fullerene-like WS2 nanocomposites containing a β-nucleating agent: Isothermal crystallization and melting behavior. *J. Phys. Chem. B* **2012**, *116*, 1788−1795.

(11) Seki, M.; Thurman, D. W.; Oberhauser, J. P.; Kornfield, J. A. 2021. Shear-Mediated Crystallization of Isotactic Polypropylene: The Role of Long Chain-Long Chain Overlap. *Macromolecules* **2002**, *35*, 2583.

(12) van der Meer, D. W. *Structure-Property Relationships in Isotactic Polypropylene*; Twente University Press, 2003.

(13) Guan, W.; Wang, J.; Zhu, X.; Lu, X. Exploration on structure and stability of polypropylene during heating and cooling processes in terms of molecular dynamics simulations. *Comput. Theor. Chem.* **2014**, *1027*, 142−150.

(14) van Gunsteren, W. F.; Dolenc, J.; Mark, A. E. Molecular simulation as an aid to experimentalists. *Curr. Opin. Struct. Biol.* **2008**, *18*, 149−153.

(15) Li, J. Basic Molecular Dynamics. In *Handbook of Materials Modeling*; Yip, S., Eds.; Springer: Dordrecht, 2005, https://doi.org/10.1007/978-1-4020-3286-8_29.

(16) von Meerwall, E.; Waheed, N.; Mattice, W. L. Effect of stereochemistry on diffusion of polypropylene melts: Comparison of simulation and experiment. *Macromolecules* **2009**, *42*, 8864−8869.

(17) Logotheti, G. E.; Theodorou, D. N. Segmental and chain dynamics of isotactic polypropylene melts. *Macromolecules* **2007**, *40*, 2235−2245.

(18) Qian, C.; Ludovice, P. J. STRESS/STRAIN ANALYSIS OF POLYMERIC MATERIALS BY MOLECULAR DYNAMICS SIMULATIONS. *Makromol. Chem., Macromol. Symp.* **1993**, *65*, 123−132.

(19) Boland, E. K.; Liu, J.; Maranas, J. K. A molecular picture of motion in polyolefins. *J. Chem. Phys.* **2010**, *132*, 144901.

(20) Kitamura, R.; Kageyama, T.; Koyanagi, J.; Ogihara, S. Estimation of biaxial tensile and compression behavior of polypropylene using molecular dynamics simulation. *Adv. Compos. Mater.* **2019**, *28*, 135−146.

(21) Kim, D. H.; Hwang, Y. T.; Kim, H. S. Investigation of Mechanical and Hygroscopic Properties for the Semi-crystalline Polypropylene Polymer Via Experiments and Molecular Dynamics. *Int. J. of Precis. Eng. and Manuf.-Green Tech.* **2021**, *8*, 177−191.

(22) Han, J.; Gee, R. H.; Boyd, R. H. Glass Transition Temperatures of Polymers from Molecular Dynamics Simulations. *Macromolecules* **1994**, *27*, 7781−7784.

(23) Yu, K. Q.; Li, Z. S.; Sun, J. Polymer structures and glass transition: A molecular dynamics simulation study. *Macromol. Theory Simul.* **2001**, *10*, 624−633.

(24) Yu, X.; Wu, R.; Yang, X. Molecular dynamics study on glass transitions in atactic-polypropylene bulk and freestanding thin films. *J. Phys. Chem. B* **2010**, *114*, 4955−4963.

(25) Schawe, J. E. K. Mobile amorphous, rigid amorphous and crystalline fractions in isotactic polypropylene during fast cooling. *J. Therm. Anal. Calorim.* **2017**, *127*, 931−937.

(26) Giordano, M.; Russo, M.; Capoluongo, P.; Cusano, A.; Nicolais, L. The effect of cooling rate on the glass transition of an amorphous polymer. *J. Non-Cryst. Solids* **2005**, *351*, 515−522.

(27) Özeren, H. D.; Guivier, M.; Olsson, R. T.; Nilsson, F.; Hedenqvist, M. S. Ranking plasticizers for polymers with atomistic simulations: PVT, mechanical properties, and the role of hydrogen bonding in thermoplastic starch. *ACS Appl. Polym. Mater.* **2020**, *2*, 2016−2026.

(28) Ingebrigtsen, T. S.; Schrøder, T. B.; Dyre, J. C. Isomorphs in model molecular liquids. *J. Phys. Chem. B* **2012**, *116*, 1018−1034.

(29) Rosenfeld, Y. Relation between the transport coefficients and the internal entropy of simple systems. *Phys. Rev. A: At., Mol., Opt. Phys.* **1977**, *15*, 2545−2549.

(30) Rosenfeld, Y. A quasi-universal scaling law for atomic transport in simple fluids. *J. Phys.: Condens. Matter* **1999**, *11*, 5415−5427.

(31) Voyiatzis, E.; Müller-Plathe, F.; Böhm, M. C. Do transport properties of entangled linear polymers scale with excess entropy? *Macromolecules* **2013**, *46*, 8710−8723.

(32) Voyiatzis, E.; Müller-Plathe, F.; Böhm, M. C. Excess entropy scaling for the segmental and global dynamics of polyethylene melts. *Phys. Chem. Chem. Phys.* **2014**, *16*, 24301−24311.

(33) Rondina, G. G.; Böhm, M. C.; Müller-Plathe, F. Predicting the Mobility Increase of Coarse-Grained Polymer Models from Excess Entropy Differences. *J. Chem. Theory Comput.* **2020**, *16*, 1431−1447.
(34) Koscher, E.; Fulchiron, R. Influence of shear on polypropylene crystallization: Morphology development and kinetics. *Polymer* **2002**, *43*, 6931−6942.
(35) Kalay, G.; Bevis, M. J. Processing and physical property relationships in injection-molded isotactic polypropylene. 1. Mechanical properties. *J. Polym. Sci., Part B: Polym. Phys.* **1997**, *35*, 241−263.
(36) Tsalikis, D. G.; Alexiou, T.; Alatas, P. V.; Mavrantzas, V. G. Shear rheology of polymer melts and nanocomposites via nonequilibrium molecular dynamics simulations. *J. Comput. Phys.* **2018**, *7*, 1.
(37) Evans, D. J.; Morriss, G. P. *Statistical Mechanics of Nonequilibrium Liquids*; ANU Press, 2007.
(38) Khan, P.; Nasir Khan, M.; Khan, N. A. Shear and cooling induced regulation of mechanical properties and glass transition temperature of isotactic polypropylene. *Mater. Today: Proc.* **2023**, *72*, 2705−2712.
(39) Lindahl, E.; Hess, B.; van der Spoel, D. GROMACS 3.0: A package for molecular simulation and trajectory analysis. *J. Mol. Model.* **2001**, *7*, 306−317.
(40) Van Der Spoel, D.; Lindahl, E.; Hess, B.; Groenhof, G.; Mark, A. E.; Berendsen, H. J. C. GROMACS: Fast, flexible, and free. *J. Comput. Chem.* **2005**, *26*, 1701−1718.
(41) Huang, J.; Mackerell, A. D. CHARMM36 all-atom additive protein force field: Validation based on comparison to NMR data. *J. Comput. Chem.* **2013**, *34*, 2135−2145.
(42) Huang, J.; Rauscher, S.; Nawrocki, G.; Ran, T.; Feig, M.; de Groot, B. L.; Grubmüller, H.; MacKerell, A. D. CHARMM36m: An improved force field for folded and intrinsically disordered proteins. *Nat. Methods* **2017**, *14*, 71−73.
(43) Berendsen, H. J. C.; Postma, J. P. M.; Van Gunsteren, W. F.; Dinola, A.; Haak, J. R. Molecular dynamics with coupling to an external bath. *J. Chem. Phys.* **1984**, *81*, 3684−3690.
(44) Parrinello, M.; Rahman, A. Polymorphic transitions in single crystals: A new molecular dynamics method. *J. Appl. Phys.* **1981**, *52*, 7182−7190.
(45) Jabbarzadeh, A.; Tanner, R. I. Flow-induced crystallization: Unravelling the effects of shear rate and strain. *Macromolecules* **2010**, *43*, 8136−8142.
(46) Nafar Sefiddashti, M. H.; Edwards, B. J.; Khomami, B. Steady shearing flow of a moderately entangled polyethylene liquid. *J. Rheol.* **2016**, *60*, 1227−1244.
(47) Pal, S.; Mitra, N.; Sarkar, P. K.; Prasad, D. Stretch-induced helix to extended coil transition of crystalline α phase isotactic polypropylene: A molecular dynamics study. *Polym. Cryst.* **2020**, *3*, No. e10143.
(48) Baig, C.; Mavrantzas, V. G.; Kröger, M. Flow effects on melt structure and entanglement network of linear polymers: Results from a nonequilibrium molecular dynamics simulation study of a polyethylene melt in steady shear. *Macromolecules* **2010**, *43*, 6886−6902.
(49) Hagita, K.; Fujiwara, S. Single-chain folding of a quenched isotactic polypropylene chain through united atom molecular dynamics simulations. *Polymer* **2019**, *183*, 121861.
(50) Lawrence Galloway, K.; et al. Scaling of relaxation and excess entropy in plastically deformed amorphous solids. *Proc. Natl. Acad. Sci. U.S.A.* **2020**, *117*, 11887.
(51) Khan, P.; Goel, G. Martini Coarse-Grained Model for Clay-Polymer Nanocomposites. *J. Phys. Chem. B* **2019**, *123*, 9011−9023.
(52) Williams, M. L.; Landel, R. F.; Ferry, J. D. The Temperature Dependence of Relaxation Mechanisms in Amorphous Polymers and Other Glass-forming Liquids. *J. Am. Chem. Soc.* **1955**, *77*, 3701−3707.
(53) Voyiatzis, E.; Müller-Plathe, F.; Böhm, M. C. Excess entropy scaling for the segmental and global dynamics of polyethylene melts. *Phys. Chem. Chem. Phys.* **2014**, *16*, 24301−24311.
(54) Dyre, J. C. Perspective: Excess-entropy scaling. *J. Chem. Phys.* **2018**, *149*, 210901.
(55) Freischmidt, H. M.; Shanks, R. A.; Moad, G.; Uhlherr, A. Characterization of polyolefin melts using the polymer reference interaction site model integral equation theory with a single-site united atom model. *J. Polym. Sci., Part B: Polym. Phys.* **2001**, *39*, 1803−1814.
(56) Boland, E. K.; Liu, J.; Maranas, J. K. A molecular picture of motion in polyolefins. *J. Chem. Phys.* **2010**, *132*, 144901.
(57) Teh, J. W.; Blom, H. P.; Rudin, A. A study on the crystallization behaviour of polypropylene, polyethylene and their blends by dynamic mechanical and thermal methods. *Polymer* **1994**, *35*, 1680−1687.
(58) Ballard, D. G. H.; Cheshire, P.; Longman, G. W.; Schelten, J. Small-angle neutron scattering studies of isotropic polypropylene. *Polymer* **1978**, *19*, 379−385.
(59) Tsamopoulos, A. J.; Katsarou, A. F.; Tsalikis, D. G.; Mavrantzas, V. G. Shear Rheology of Unentangled and Marginally Entangled Ring Polymer Melts from Large-Scale Nonequilibrium Molecular Dynamics Simulations. *Polymers* **2019**, *11*, 1194.
(60) Yamamoto, T.; Sawada, K. Molecular-dynamics simulation of crystallization in helical polymers. *J. Chem. Phys.* **2005**, *123*, 234906.
(61) Heine, D.; Wu, D. T.; Curro, J. G.; Grest, G. S. Role of intramolecular energy on polyolefin miscibility: Isotactic polypropylene/polyethylene blends. *J. Chem. Phys.* **2003**, *118*, 914−924.
(62) Nagarajan, K.; Myerson, A. S. Molecular Dynamics of Nucleation and Crystallization of Polymers. *Cryst. Growth Des.* **2001**, *1*, 131−142.
(63) Goel, G.; Krekelberg, W. P.; Errington, J. R.; Truskett, T. M. Tuning density profiles and mobility of inhomogeneous fluids. *Phys. Rev. Lett.* **2008**, *100*, 106001.
(64) Glüge, R.; Altenbach, H.; Kolesov, I.; Mahmood, N.; Beiner, M.; Androsch, R. On the effective elastic properties of isotactic polypropylene. *Polymer* **2019**, *160*, 291−302.
(65) Phulkerd, P.; Funahashi, Y.; Ito, A.; Iwasaki, S.; Yamaguchi, M. Perpendicular orientation between dispersed rubber and polypropylene molecules in an oriented sheet. *Polym. J.* **2018**, *50*, 309−318.
(66) Batista, N. L.; Olivier, P.; Bernhart, G.; Rezende, M. C.; Botelho, E. C. Correlation between degree of crystallinity, morphology and mechanical properties of PPS/carbon fiber laminates. *Mater. Res.* **2016**, *19*, 195−201.
(67) Hassani, F.; Martin, P. J.; Falzon, B. G. Investigation on the effect of cooling rate on the mechanical properties of polypropylene self-reinforced composites. *ECCM 2018—18th European Conference on Composite Materials*, 2019.
(68) Hossain, D.; Tschopp, M.; Ward, D.; Bouvard, J.; Wang, P.; Horstemeyer, M. Molecular dynamics simulations of deformation mechanisms of amorphous polyethylene. *Polymer* **2010**, *51*, 6071−6083.
(69) Shang, Y.; Zhang, X.; Xu, H.; Li, J.; Jiang, S. Microscopic study of structure/property interrelation of amorphous polymers during uniaxial deformation: A molecular dynamics approach. *Polymer* **2015**, *77*, 254−265.
(70) Vu-Bac, N.; Lahmer, T.; Keitel, H.; Zhao, J.; Zhuang, X.; Rabczuk, T. Stochastic predictions of bulk properties of amorphous polyethylene based on molecular dynamics simulations. *Mech. Mater.* **2014**, *68*, 70−84.
(71) Sarangapani, R.; Reddy, S. T.; Sikder, A. K. Molecular dynamics simulations to calculate glass transition temperature and elastic constants of novel polyethers. *J. Mol. Graphics Modell.* **2015**, *57*, 114−121.
(72) Pearce, E. M. Introduction to polymer science and technology: An SPE text-book, Herman S. Kaufman and Joseph J. Falcetta, Eds., Wiley-Interscience, New York, 1977, 613 pp., $27.50. *J. Polym. Sci., Polym. Lett. Ed.* **1978**, *16*, 55.
(73) Sakai, A.; Tanaka, K.; Kajiyama, T.; Takahara, A. Thermal molecular motion at surface of atactic polypropylene films. *Polymer* **2002**, *43*, 5109−5115.
(74) He, J.; Liu, W.; Huang, Y. X. Simultaneous determination of glass transition temperatures of several polymers. *PLoS One* **2016**, *11*, No. e0151454.

https://doi.org/10.1021/acsomega.3c03378
ACS Omega 2023, 8, 36775−36788

(75) Buchholz, J.; Paul, W.; Varnik, F.; Binder, K. Cooling rate dependence of the glass transition temperature of polymer melts: Molecular dynamics study. *J. Chem. Phys.* **2002**, *117*, 7364−7372.
(76) Bao, Q.; Yang, Z.; Lu, Z. Molecular dynamics simulation of amorphous polyethylene (PE) under cyclic tensile-compressive loading below the glass transition temperature. *Polymer* **2020**, *186*, 121968.
(77) Peyser, P.; Bascom, W. D. Effect of Filler and Cooling Rate on the Glass Transition of Polymers. *J. Macromol. Sci., Part B: Phys* **1977**, *13*, 597−610.
(78) Hu, Y.; Liao, Y.; Zheng, Y.; Ikeda, K.; Okabe, R.; Wu, R.; Ozaki, R.; Xu, J.; Xu, Q. Influence of Cooling Rate on Crystallization Behavior of Semi-Crystalline Polypropylene: Experiments and Mathematical Modeling. *Polymers* **2022**, *14*, 3646.
(79) Scott Bair, C. M. *An introduction to the rheology of polymeric liquids*; *Tribology and Interface Engineering Series*; Elsevier, 2007; Vol. *54*, pp 15−34.
(80) Vincent, R.; Langlotz, M.; Düngen, M. Viscosity measurement of polypropylene loaded with blowing agents (propane and carbon dioxide) by a novel inline method. *J. Cell. Plast.* **2020**, *56*, 73−88.
(81) Yucel, T.; Cebe, P.; Kaplan, D. L. Vortex-induced injectable silk fibroin hydrogels. *Biophys. J.* **2009**, *97*, 2044−2050.
(82) Nagy, D.; Belina, K. Measuring viscosity of polyethylene blends using a rotational rheometer. *J. Phys.: Conf. Ser.* **2018**, *1045*, 012030.
(83) Kumar, N. G. Viscosity-molecular weight-temperature-shear rate relationships of polymer melts: A literature review. *J. Polym. Sci., Part D: Macromol. Rev.* **1980**, *15*, 255−325.
(84) Meng, L.; Wu, D.; Kelly, A.; Woodhead, M.; Liu, Y. Experimental investigation of the rheological behaviors of polypropylene in a capillary flow. *J. Appl. Polym. Sci.* **2016**, *133*, 43459.
(85) Bonnecaze, R. T.; Khabaz, F.; Mohan, L.; Cloitre, M. Excess entropy scaling for soft particle glasses. *J. Rheol.* **2020**, *64*, 423−431.
(86) Krekelberg, W. P.; Ganesan, V.; Truskett, T. M. Shear-rate-dependent structural order and viscosity of a fluid with short-range attractions. *Phys. Rev. E: Stat., Nonlinear, Soft Matter Phys.* **2008**, *78*, 010201.
(87) Krekelberg, W. P.; Ganesan, V.; Truskett, T. M. Structural signatures of mobility on intermediate time scales in a supercooled fluid. *J. Chem. Phys.* **2010**, *132*, 184503.
(88) Ingebrigtsen, T. S.; Tanaka, H. Structural predictor for nonlinear sheared dynamics in simple glass-forming liquids. *Proc. Natl. Acad. Sci. U.S.A.* **2018**, *115*, 87−92.
(89) Krekelberg, W. P.; Truskett, T. M.; Ganesan, V. Relationship between shear viscosity and structure of a model colloidal suspension. *Chem. Eng. Commun.* **2009**, *197*, 63−75.

https://doi.org/10.1021/acsomega.3c03378
ACS Omega 2023, 8, 36775−36788